

A COMBINED MODEL FOR A BUCKET BRIGADE DEVICE AND ITS INPUT AND OUTPUT FILTERS

Martin Holters

Department of Signal Processing and Communication
 Helmut Schmidt University
 Hamburg, Germany
 martin.holters@hsu-hh.de

Julian D. Parker

Native Instruments GmbH
 Berlin, Germany
 julian.parker@native-instruments.com

ABSTRACT

Bucket brigade devices (BBDs) were invented in the late 1960s as a method of introducing a time-delay into an analog electrical circuit. They work by sampling the input signal at a certain clock rate and shifting it through a chain of capacitors to obtain the delay. BBD chips have been used to build a large variety of analog effects processing devices, ranging from chorus to flanging to echo effects. They have therefore attracted interest in virtual analog modeling and a number of approaches to modeling them digitally have appeared. In this paper, we propose a new model for the bucket-brigade device. This model is based on a variable sample-rate, and utilizes the surrounding filtering circuitry found in real devices to avoid the need for the interpolation usually needed in such a variable sample-rate system.

1. INTRODUCTION

Bucket brigade devices (BBDs) were invented in the late 1960s at Philips Research Labs [1], as a method of introducing a time-delay into an analog electrical circuit. These chips were subsequently used to build a large variety of analog effects processing devices, ranging from chorus to flanging to echo effects. Well-known BBD-based devices include the Memory Man delay/echo pedal and the Electric Mistress flanger effect from Electro-Harmonix, as well as a series of chorus designs produced by Roland, starting in the mid 70s with the chorus circuit of the JC-120 amplifier and culminating with the Dimension-D rack unit and the chorus included in the Juno-60 synthesizer.

There have been a number of approaches to modeling BBD devices digitally. Raffel [2] concentrated on the filtering and non-linear behavior of the BBD, without treating the dynamic behavior of the BBD when the clock-rate is varied. Huovilainen [3] and Mačák [4] both model the BBD in the context of a flanger effect. The latter uses a variable sample rate delay to model the BBD delay behavior, whilst the former uses a method based on storing the times at which an input arrived to the BBD. Variable sample rate digital delay-lines have been described in the past, primarily for the use in physical models of acoustic systems [5]. Recently, methods have been proposed for emulating tape and BBD-like behaviour by storing the previous 'speed' of the system (clock-rate in a BBD) [6].

The presented technique is built on the observation that BBD chips, due to their sampling nature, are typically used in conjunction with low-pass filters to prevent aliasing. We propose a novel approach, modeling the BBD together with these filters. The BBD itself will be trivially modeled as what it is: a fixed length but variable sample rate delay-line. The main novelty of the proposed approach is that the resampling between the audio sampling rate and the variable BBD clock rate utilizes the filters already present

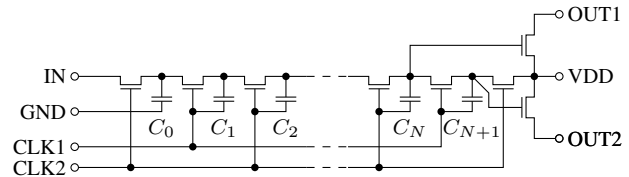


Figure 1: Simplified BBD schematic

in the analog circuit and hence avoids the need for additional interpolation. The lack of direct interpolation results in more accurate fitting of the frequency response of the circuit as no additional filtering is introduced from the interpolation. Additionally, the distortion produced by the constant variation of the interpolation filter is avoided. Experimental results confirm that the method leads to a faithful BBD model.

2. WORKING PRINCIPLE OF BUCKET BRIGADE DEVICES

Figure 1 shows a simplified schematic of a typical BBD. We have omitted additional field effect transistors that, together with the shown ones, form tetrodes to reduce unwanted coupling between the stages. While we leave the detailed explanation of the propagation principle to [1] and the reason for using tetrodes to [7], we shall briefly look at the input and output circuitry.

While the input transistor, controlled by CLK2, is open, capacitor C₀ follows the input voltage $u_{\text{BBD}}(t)$ between the IN and GND terminals. Closing the input transistor hence corresponds to sampling the input signal at the time instant t_0 of the respective clock edge. The two clock signals CLK1 and CLK2 are complementary, so that the transistor connecting C₀ and C₁ opens (nearly) in the same instant and the signal sample $u_{\text{BBD}}(t_0)$ is transferred to C₁ while C₀ returns to the reference voltage [1].

Let the following clock edges occur at times t_1, t_2, \dots . Note that only at every second clock edge t_n, n even, the input transistor transitions from open to closed, sampling the input. Thus at any time, only half the capacitors carry the signal, while the others are at the reference voltage. In the metaphor of the bucket brigade, this corresponds to half the buckets being filled with water and transported in one direction, while the other half is empty and is transported back (to be filled again).

With every edge, the charge representing the signal is propagated to the next capacitor, that is after the clock edge at t_n , capacitor C_{n+1} holds $u_{\text{BBD}}(t_0)$. It follows that the signal arrives at capacitor C_N at t_{N-1} and drives the first output terminal OUT1 while the second output terminal OUT2 is in high impedance state.

After the next clock edge at t_N , capacitor C_{N+1} holds $u_{\text{BBD}}(t_0)$ and drives OUT2 while OUT1 is in high impedance state. This continues until at t_{N+1} , the next signal sample $u_{\text{BBD}}(t_2)$ arrives at capacitor C_N and drives OUT1 while OUT2 is in high impedance state again. Therefore, application circuits combine the two outputs, so that the signal sampled at t_0 is present at the combined output from t_{N-1} to t_{N+1} , that is

$$y_{\text{BBD}}(t) = u_{\text{BBD}}(t_n) \text{ for } t_{n+N-1} \leq t < t_{n+N+1}, n \text{ even.} \quad (1)$$

In other words, for a constant clock rate, the signal is not only delayed by $N/2$ clock periods (corresponding to N clock edges). It is also convolved with a rectangular pulse of one clock period width giving rise to a high-frequency attenuation depending on the BBD clock rate. For all commercially available BBDs, N is even, so that if the input sampling occurs at every t_n , n even, the output changes its value at every t_n , n odd, which we will assume for simplicity during the development of the proposed model.

In addition to the desired functionality of delaying the signal, due to their analog nature, BBD chips usually also alter the signal in unwanted ways. In particular, the long chain of active semiconductor stages acting upon the signal typically adds noise and may introduce non-linear distortions. Additionally, losses and tolerances in the capacitances may lead to non-unity overall gain. However, this paper focuses on the sampling and delay behavior and does not consider these parasitic effects.

Finally, as a direct consequence of the working principle, there are several inherent sources of aliasing distortion in the BBD system – firstly there are frequency components present at the input of the BBD that exceed the effective Nyquist frequency of the BBD. These components will be reflected around the BBD Nyquist frequency. Most BBD circuits include a filter at the input to suppress this behavior. Secondly, there are the image-spectra created by sample-and-hold nature of the output of the BBD chip. Similarly to at the input, most BBD circuits include an output filter to suppress these images. These types of aliasing (at least when present in small quantities) can be considered to be desirable for the expected sound of a BBD and should be reproduced by a digital model.

3. PROPOSED MODEL

We propose to model the BBD as a delay-line of fixed length, operating at another, potentially varying sampling rate, the BBDs clock rate, similar to [4]. However, instead of using simple interpolation for the necessary sampling rate conversions, we will exploit the fact that typical application circuits contain low-pass filters at the BBDs input and output. These are responsible to prevent aliasing from the sampling and reconstruction process of the BBD. We will make use of exactly these anti-aliasing filters for the necessary resampling. The transformation of these filters to the digital domain will be carried out using a modified impulse-invariant transform similar to the approach taken in [8], as this facilitates dealing with different, asynchronous sampling rates on input and output side.

3.1. Input filter

Perfect reconstruction of the analog signal $u(t)$ from its samples $\bar{u}(k) = u(kT_s)$, where $T_s = 1/f_s$ is the sampling interval, can be understood as subjecting a train of Dirac impulses weighted with $\bar{u}(k) \cdot T_s$ to an ideal low-pass filter, band-limiting it to the Nyquist frequency. Here, we replace the ideal low-pass filter with the input low-pass filter $H_{\text{in}}(s)$ found in front of the BBD, which

is assumed to have sufficient attenuation at the Nyquist frequency (of the original audio sampling rate f_s) that an acceptable amount of aliasing remains. Our aim is to obtain samples $u_{\text{BBD}}(t_n)$ of the filter's output (being the BBD's input) at times t_n , n even, at which the BBD samples its input.

Let $H_{\text{in}}(s)$ be expanded into partial fractions as

$$H_{\text{in}}(s) = \sum_{m=1}^{M_{\text{in}}} \frac{r_{\text{in},m}}{s - p_{\text{in},m}} \quad (2)$$

where we may assume no non-negative powers of s to occur as $H_{\text{in}}(s)$ is a low-pass filter and further assume all poles $p_{\text{in},m}$ to be simple to simplify the following development. Then the corresponding impulse response can easily be found to be

$$h_{\text{in}}(t) = \begin{cases} \sum_{m=1}^{M_{\text{in}}} r_{\text{in},m} \cdot e^{p_{\text{in},m}t} & \text{for } t \geq 0 \\ 0 & \text{otherwise.} \end{cases} \quad (3)$$

Exciting the filter with a single Dirac impulse weighted with $\bar{u}(k) \cdot T_s$ at time kT_s , we obtain the corresponding output

$$u_{\text{BBD},k}(t) = \begin{cases} \bar{u}(k) \cdot T_s \sum_{m=1}^{M_{\text{in}}} r_{\text{in},m} \cdot e^{p_{\text{in},m}(t-kT_s)} & \text{if } t \geq kT_s \\ 0 & \text{otherwise.} \end{cases} \quad (4)$$

Now let the time be decomposed as $t = (l_n + d_n)T_s$ where l_n is an integer and $0 \leq d_n < 1$. Then

$$u_{\text{BBD},k}((l_n + d_n)T_s) = \begin{cases} \bar{u}(k) \sum_{m=1}^{M_{\text{in}}} g_{\text{in},m}(d_n) \cdot \bar{p}_{\text{in},m}^{l_n-k} & \text{if } l_n \geq k \\ 0 & \text{otherwise} \end{cases} \quad (5)$$

where $\bar{p}_{\text{in},m} = e^{p_{\text{in},m}T_s}$ and

$$g_{\text{in},m}(d_n) = T_s \cdot r_{\text{in},m} \cdot \bar{p}_{\text{in},m}^{d_n}. \quad (6)$$

Further rewriting as

$$u_{\text{BBD},k}((l_n + d_n)T_s) = \sum_{m=1}^{M_{\text{in}}} g_{\text{in},m}(d_n) \cdot x_{\text{in},m,k}(l_n) \quad (7)$$

with

$$x_{\text{in},m,k}(l_n) = \begin{cases} \bar{u}(k) \cdot \bar{p}_{\text{in},m}^{l_n-k} & \text{if } l_n \geq k \\ 0 & \text{otherwise,} \end{cases} \quad (8)$$

we see that the latter can be expressed recursively as

$$x_{\text{in},m,k}(l_n) = \begin{cases} \bar{p}_{\text{in},m} \cdot x_{\text{in},m,k}(l_n - 1) & \text{if } l_n > k \\ \bar{u}(k) & \text{if } l_n = k \\ 0 & \text{otherwise.} \end{cases} \quad (9)$$

Now by the superposition principle, the filter response to the complete input signal is given by

$$u_{\text{BBD}}((l_n + d_n)T_s) = \sum_k u_{\text{BBD},k}((l_n + d_n)T_s) = \sum_{m=1}^{M_{\text{in}}} g_{\text{in},m} \cdot x_{\text{in},m}(l_n) \quad (10)$$

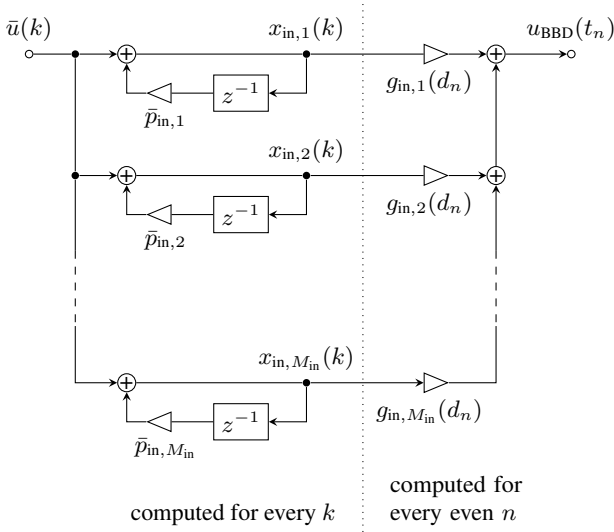


Figure 2: Digital realization of the input filter where $t_n = (k + d_n) \cdot T_s$, n even, are the sampling instants of the BBD input

where

$$x_{in,m}(l_n) = \sum_k x_{in,m,k}(l_n) = \bar{p}_{in,m} \cdot x_{in,m}(l_n - 1) + \bar{u}(l_n) \quad (11)$$

constitutes a simple first-order recursive filter. This leads to the digital realization shown in figure 2. For every input sample $\bar{u}(k)$, the parallel recursive parts are updated, and for every sample needed at the BBD input, the weighted sum is evaluated. The weights of the latter depend on the fractional offset d_n of the BBD sampling instant t_n within the audio rate sampling interval.

3.2. Output filter

The development for the output filter is similar but differs in two aspects: Now, the input samples occur at the BBD clock rate while the output samples are needed at the fixed audio sampling rate, and the input samples have to be treated as consecutive rectangular pulses instead of Dirac impulses. That is, $y_{BBD}(t)$ is piecewise constant in intervals $[t_n, t_{n+2})$, n odd.

For the following development, it is helpful to work with a sequence of differences $\Delta(n) = y_{BBD}(t_n) - y_{BBD}(t_{n-1})$, n odd, with associated step functions

$$\epsilon_n(t) = \begin{cases} \Delta(n) & \text{if } t \geq t_n \\ 0 & \text{otherwise} \end{cases} \quad (12)$$

such that

$$y_{BBD}(t) = \sum_n \epsilon_n(t). \quad (13)$$

Similar to the previous development, we first determine the filter output produced by a single step $\epsilon_n(t)$ and consider the output filter $H_{out}(s)$ to be decomposed into partial fractions as

$$H_{out}(s) = \sum_{m=1}^{M_{out}} \frac{r_{out,m}}{s - p_{out,m}}. \quad (14)$$

The response to a unit step (Heaviside step function) is

$$h_{out}(t) = \begin{cases} \sum_{m=1}^{M_{out}} \frac{r_{out,m}}{p_{out,m}} (e^{p_{out,m}t} - 1) & \text{if } t \geq 0 \\ 0 & \text{otherwise} \end{cases} \quad (15)$$

$$= \begin{cases} H_0 + \sum_{m=1}^{M_{out}} \frac{r_{out,m}}{p_{out,m}} e^{p_{out,m}t} & \text{if } t \geq 0 \\ 0 & \text{otherwise} \end{cases} \quad (16)$$

where $H_0 = -\sum_{m=1}^{M_{out}} \frac{r_{out,m}}{p_{out,m}}$. It follows trivially that the response $y_n(t)$ to a single $\epsilon_n(t)$ is

$$y_n(t) = \begin{cases} H_0 \Delta(n) + \Delta(n) \sum_{m=1}^{M_{out}} \frac{r_{out,m}}{p_{out,m}} e^{p_{out,m}(t-t_n)} & \text{if } t \geq t_n \\ 0 & \text{otherwise.} \end{cases} \quad (17)$$

Now let $\bar{y}_n(k) = y_n(kT_s)$ be samples of the individual responses taken at the original audio sampling rate, and $t_n = (l_n - 1 + d_n)T_s$, where l_n is an integer and $0 < d_n \leq 1$. Then

$$\bar{y}_n(k) = \begin{cases} H_0 \Delta(n) + \Delta(n) \sum_{m=1}^{M_{out}} \frac{r_{out,m}}{p_{out,m}} \bar{p}_{out,m}^{k-l_n+1-d_n} & \text{if } k \geq l_n \\ 0 & \text{otherwise} \end{cases} \quad (18)$$

where $\bar{p}_{out,m} = e^{p_{out,m}T_s}$. We further rewrite as

$$\bar{y}_n(k) = \sum_{m=1}^{M_{out}} x_{out,m,n}(k) + \begin{cases} H_0 \Delta(n) & \text{if } k \geq l_n \\ 0 & \text{otherwise} \end{cases} \quad (19)$$

with

$$x_{out,m,n}(k) = \begin{cases} \bar{p}_{out,m}^{k-l_n} g_{out,m}(d_n) \Delta(n) & \text{if } k \geq l_n \\ 0 & \text{otherwise} \end{cases} \quad (20)$$

where

$$g_{out,m}(d_n) = \frac{r_{out,m}}{p_{out,m}} \bar{p}_{out,m}^{1-d_n}. \quad (21)$$

Similar to the input filter, we can express this using the recursion

$$x_{out,m,n}(k) = \begin{cases} \bar{p}_{out,m} \cdot x_{out,m,n}(k-1) & \text{if } k > l_n \\ g_{out,m}(d_n) \Delta(n) & \text{if } k = l_n \\ 0 & \text{otherwise} \end{cases} \quad (22)$$

and by superimposing all input step functions get the recursive first order subsystem

$$x_{out,m}(k) = \sum_n x_{out,m,n}(k) = \bar{p}_{out,m} \cdot x_{out,m}(k-1) + \sum_{k=l_n}^n g_{out,m}(d_n) \Delta(n) \quad (23)$$

where the driving term includes all steps occurring during the past sampling interval, that is all odd n such that $(k-1)T_s < t_n \leq kT_s$. Further, by definition

$$H_0 \sum_{l_n \leq k} \Delta(n) = H_0 y_{BBD}(kT_s). \quad (24)$$

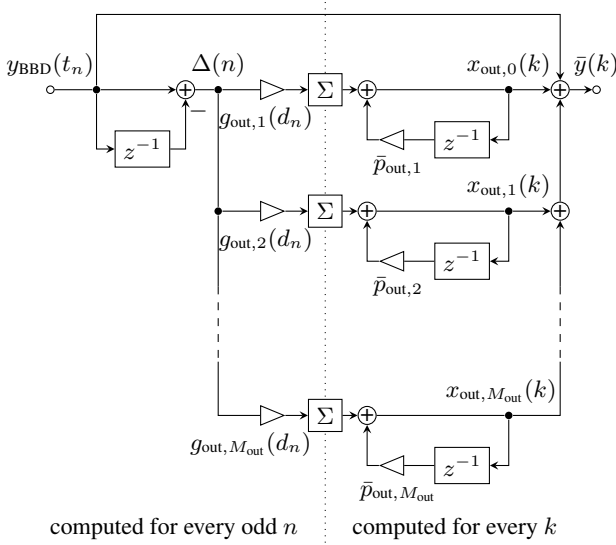


Figure 3: Digital realization of the output filter where $t_n = (k - 1 + d_n) \cdot T_s$, n odd, are the switching instants of the BBD output

The final output then is the sum of these first-order subsystems, i.e.

$$y(k) = H_0 y_{\text{BBD}}(kT_s) + \sum_{m=1}^{M_{\text{out}}} x_{\text{out},m}(k), \quad (25)$$

leading to the digital realization shown in figure 3, where the Σ -nodes on the border between the sampling rates shall denote the accumulation of the inputs on the n side over one interval of the k side.

Algorithm 1 shows pseudo code for the complete model of BBD and filters. Note that the inner loop (lines 6–19), which performs the operations running at the BBD clock rate, is executed before the k -th input sample $\bar{u}(k)$ is processed in line 21, and therefore effectively does the processing for the time interval between the $k - 1$ -th and k -th sample. The BBD samples are assumed to be stored in a queue of fixed length N , accessed with `enqueue()` and `dequeue()` to insert and retrieve a sample, respectively.

3.3. Real-valued systems

In above derivation, all coefficients are potentially complex-valued. Of course, unless they are already real, they occur in conjugate complex pairs, so that two complex-valued first-order systems can be combined into one real-valued second-order system. The calculation is straight-forward and we only present the resulting equivalent sub-systems in figures 4 and 5, where the m -th and \hat{m} -th pole are assumed to form a conjugate pair and the (real-valued) coefficients for the formed input-filter sub-system are given by

$$a_{1,\text{in},m} = 2 \cos(\angle \bar{p}_{\text{in},m}) \quad (26)$$

$$a_{2,\text{in},m} = -|\bar{p}_{\text{in},m}|^2 \quad (27)$$

$$b_{0,\text{in},m}(d_n) = \beta_{\text{in},m} \cdot |\bar{p}_{\text{in},m}|^{d_n} \cdot \cos(\angle r_{\text{in},m} + d_n \angle \bar{p}_{\text{in},m}) \quad (28)$$

$$b_{1,\text{in},m}(d_n) = -\beta_{\text{in},m} \cdot |\bar{p}_{\text{in},m}|^{d_n+1} \cdot \cos(\angle r_{\text{in},m} + (d_n - 1) \angle \bar{p}_{\text{in},m}) \quad (29)$$

where $\beta_{\text{in},m} = 2T_s \cdot |r_{\text{in},m}|$. Similarly, the coefficients for the

Algorithm 1 Proposed BBD and filters model

```

1:  $n \leftarrow 0$ 
2:  $x_{\text{in},m} \leftarrow 0$  for  $m = 1, \dots, M_{\text{in}}$ 
3:  $x_{\text{out},m} \leftarrow 0$  for  $m = 1, \dots, M_{\text{out}}$ 
4:  $y_{\text{BBD},\text{old}} \leftarrow 0$ 
5: for all  $k$  do
6:   while  $t_n < kT_s \vee (n \text{ odd} \wedge t_n = kT_s)$  do
7:      $d_n \leftarrow t_n - (k - 1)T_s$ 
8:     if  $n$  even then
9:       enqueue( $\sum_{m=1}^{M_{\text{in}}} g_{\text{in},m}(d_n) \cdot x_{\text{in},m}$ )
10:    else
11:       $y_{\text{BBD}} \leftarrow$  dequeue()
12:       $\Delta \leftarrow y_{\text{BBD}} - y_{\text{BBD},\text{old}}$ 
13:       $y_{\text{BBD},\text{old}} \leftarrow y_{\text{BBD}}$ 
14:      for  $m \in 1, \dots, M_{\text{out}}$  do
15:         $x_{\text{out},m} \leftarrow x_{\text{out},m} + g_{\text{out},m}(d_n) \cdot \Delta$ 
16:      end for
17:    end if
18:     $n \leftarrow n + 1$ 
19:  end while
20:  for  $m \in 1, \dots, M_{\text{in}}$  do
21:     $x_{\text{in},m} \leftarrow \bar{p}_{\text{in},m} x_{\text{in},m} + \bar{u}(k)$ 
22:  end for
23:   $y(k) = H_0 \cdot y_{\text{BBD},\text{old}} + \sum_{m=0}^{M_{\text{out}}} x_{\text{out},m}(k)$ 
24:  for  $m \in 1, \dots, M_{\text{out}}$  do
25:     $x_{\text{out},m} \leftarrow \bar{p}_{\text{out},m} x_{\text{out},m}$ 
26:  end for
27: end for
    
```

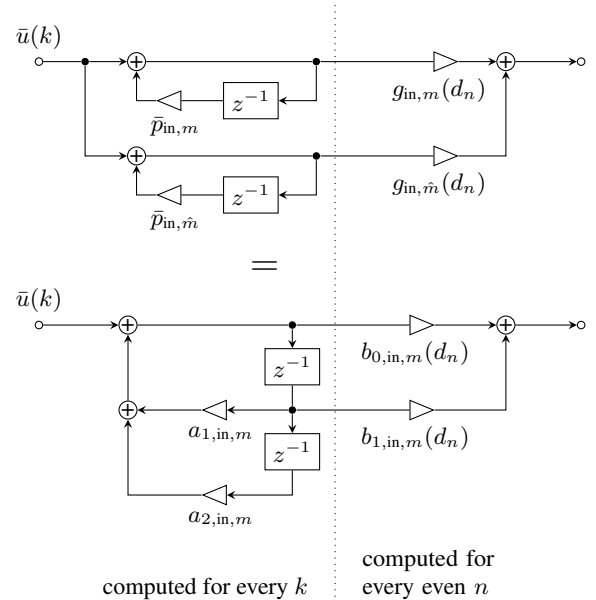


Figure 4: Two complex-valued first-order systems for a conjugate complex pole pair of the input filter and the equivalent real-valued second-order system

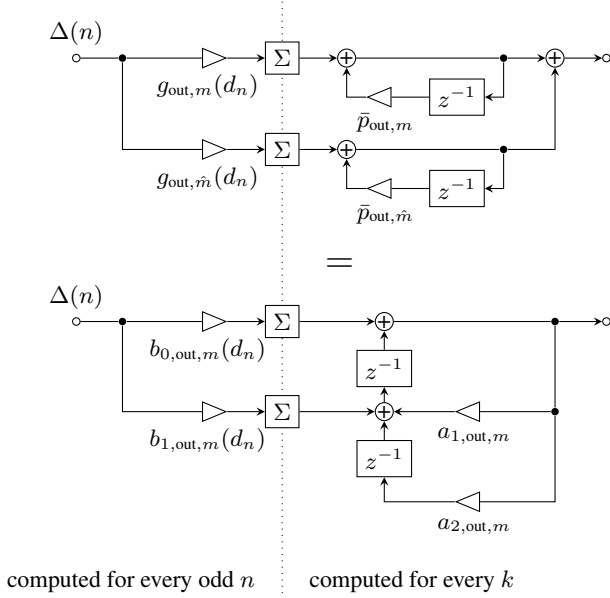


Figure 5: Two complex-valued first-order systems for a conjugate complex pole pair of the output filter and the equivalent real-valued second-order system

formed output-filter sub-system are given by

$$a_{1,\text{out},m} = 2 \cos(\angle \bar{p}_{\text{out},m}) \quad (30)$$

$$a_{2,\text{out},m} = -|\bar{p}_{\text{out},m}|^2 \quad (31)$$

$$b_{0,\text{out},m}(d_n) = \beta_{\text{out},m} \cdot |\bar{p}_{\text{out},m}|^{1-d_n} \cdot \cos(\angle r_{\text{out},m} + (1-d_n)\angle \bar{p}_{\text{out},m}) \quad (32)$$

$$b_{1,\text{out},m}(d_n) = -\beta_{\text{out},m} \cdot |\bar{p}_{\text{out},m}|^{2-d_n} \cdot \cos(\angle r_{\text{out},m} - d_n \angle \bar{p}_{\text{out},m}) \quad (33)$$

where $\beta_{\text{out},m} = 2 \left| \frac{r_{\text{out},m}}{p_{\text{out},m}} \right|$. Note that by precomputing constants and reusing common terms, computing the b coefficients for one second-order sub-system requires evaluation of one exponential and two cosine functions. Alternatively, given the limited range of d_n , one may use polynomial approximations or look-up tables for the b coefficients. An analysis of the effects of approximation errors is beyond the scope of this paper, however.

4. RESULTS

In the following, we consider the BBD and filter combination as found in the chorus effect of the Juno-60 synthesizer. As a detailed circuit analysis is beyond the scope of this paper, we only state the relevant aspects. Both the input and output filter are sixth-order filters that can be decomposed into a first-order high-pass filter (for adjusting bias voltages) and a fifth-order low-pass filter. We will only include the latter in our combined BBD/filter model. Numerical circuit analysis gives the coefficients of table 1, corresponding to the frequency responses shown in figure 6.

We first validate the model by studying a situation where we can analytically derive the expected output: sinusoidal input and a BBD clock with constant rate f_{BBD} so that the time interval between

Table 1: Coefficients of the input and output filters

	H_{in}	H_{out}
r_1	251 589	5092
r_2	$-130\,428 - 4165i$	$11\,256 - 99\,566i$
r_3	$-130\,428 + 4165i$	$11\,256 + 99\,566i$
r_4	$4634 - 22\,873i$	$-13\,802 - 24\,606i$
r_5	$4634 + 22\,873i$	$-13\,802 + 24\,606i$
p_1	$-46\,580$	$-176\,261$
p_2	$-55\,482 + 25\,082i$	$-51\,468 + 21\,437i$
p_3	$-55\,482 - 25\,082i$	$-51\,468 - 21\,437i$
p_4	$-26\,292 - 59\,437i$	$-26\,276 - 59\,699i$
p_5	$-26\,292 + 59\,437i$	$-26\,276 + 59\,699i$

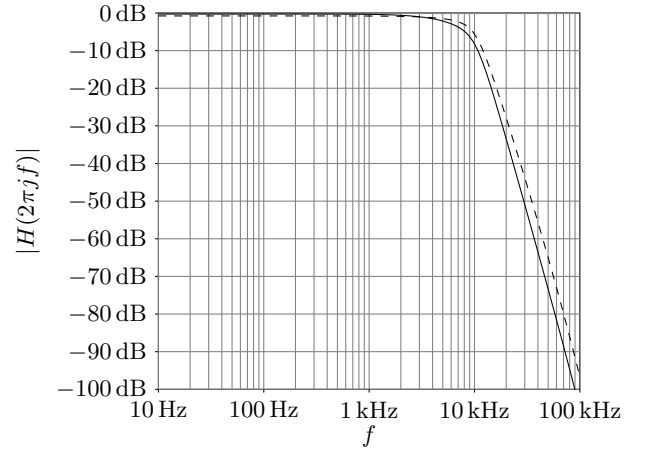


Figure 6: Frequency response of the input filter (—) and output filter (---)

two clock edges is $t_n - t_{n-1} = \frac{1}{2f_{\text{BBD}}}$, where we assume the clock to have 50% duty cycle, i.e. $t_n - t_{n-1} = t_{n-1} - t_{n-2}$, as is typical in BBD applications. For signals band-limited to $f_{\text{BBD}}/2$ and ignoring aliasing distortion introduced by the BBD, the BBD may then be treated as the linear filter

$$H_{\text{BBD}}(i\omega) = e^{-i\omega \frac{N}{2f_{\text{BBD}}}} \cdot \text{sinc}\left(\frac{\omega}{2\pi f_{\text{BBD}}}\right) \quad (34)$$

where N is the number of stages of the BBD and $\text{sinc}(x) = \frac{\sin(\pi x)}{\pi x}$. The first factor is the phase shift due to the delay, the second factor the amplitude distortion due to presenting rectangular pulses at the output. For the input signal

$$u(k) = \sin\left(2\pi \frac{f_0}{f_s} k\right) \quad (35)$$

we therefore expect the output

$$y(k) = a \cdot \sin\left(2\pi \frac{f_0}{f_s} k + \varphi\right) \quad (36)$$

where

$$a = \text{sinc}\left(\frac{f_0}{f_{\text{BBD}}}\right) \cdot |H_{\text{in}}(2\pi i f_0)| \cdot |H_{\text{out}}(2\pi i f_0)| \quad (37)$$

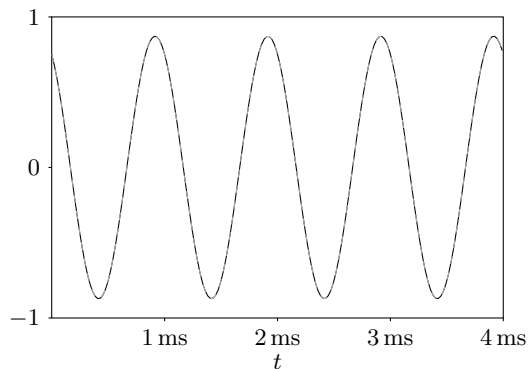
$$\varphi = -\pi f_0 \frac{N}{f_{\text{BBD}}} + \angle H_{\text{in}}(2\pi i f_0) + \angle H_{\text{out}}(2\pi i f_0). \quad (38)$$

This expected output is compared in figure 7 with the output computed using the proposed model. Here, we choose $f_0 = 1$ kHz, $f_s = 44.1$ kHz, $N = 256$, and $f_{\text{BBD}} = 50$ kHz. As can be seen, model output and theoretically expected output are in good agreement, small differences remain however. These are caused by aliasing due to the non-perfect attenuation of the filters at and above the Nyquist frequency. Figure 8 shows the same configuration, but with an instant step in f_{BBD} occurring at $t = 5$ ms. A smooth change in the frequency of the output can be seen, as is expected for a BBD. This is in contrast to a simple digital delay-line, which would exhibit a discontinuity at the output when subjected to a discontinuous change in delay time. This behaviour arises because the effective pitch of the output of the BBD compared to its input depends on the ratio of f_{BBD} between the instant when the signal was sampled by the BBD and when it exits the BBD.

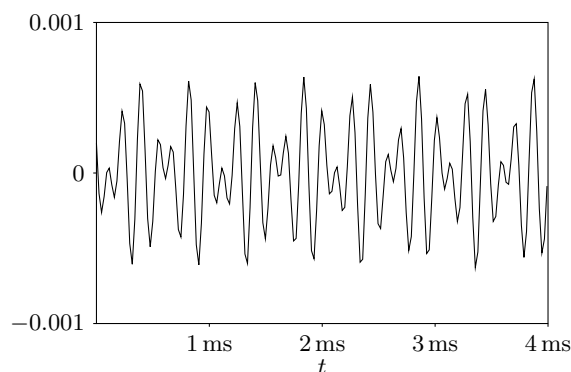
As a more practically relevant scenario, we compare the model output to the output of the BBD output filter recorded from a real Juno-60 synthesizer. The BBD clock period is controlled by a triangular LFO signal, leading to piecewise constant pitch shifts, alternatingly upwards and downwards. It is worth noting that the minimum BBD clock rate is about 26 kHz, so that the analog circuit may already introduce aliasing distortion itself, as discussed previously.

To allow a meaningful comparison, several extra considerations are necessary:

- The first-order high-pass filters previously omitted have to be included. This is done by converting them to digital filters using the bilinear transform and applying them to the input signal before and the output signal after running the BBD model.
- Measurements in the circuit showed that the BBD amplifies the signal by approximately 2.3 dB which is also included in the simulation.



(a) Output of the proposed model (—) and the theoretically expected output (---)



(b) Difference between proposed model output and theoretically expected output

Figure 7: Comparison of the output of the proposed model and theoretically expected output for a sinusoid at $f_0 = 1$ kHz sampled at $f_s = 44.1$ kHz delayed by a BBD with $N = 256$ stages clocked at $f_{\text{BBD}} = 50$ kHz

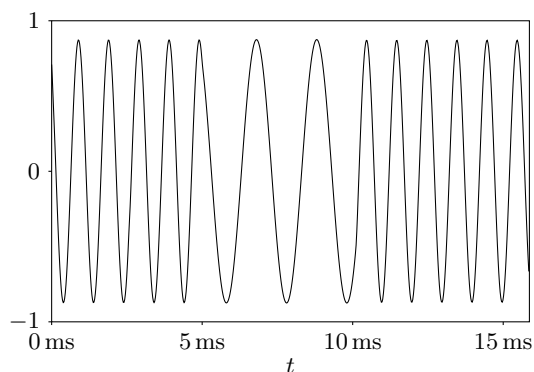


Figure 8: Model output (—) for a sinusoid of $f_0 = 1$ kHz sampled at $f_s = 44.1$ kHz delayed by a BBD with $N = 256$ stages clocked at $f_{\text{BBD}} = 50$ kHz before $t = 5$ ms and $f_{\text{BBD}} = 25$ kHz afterwards.

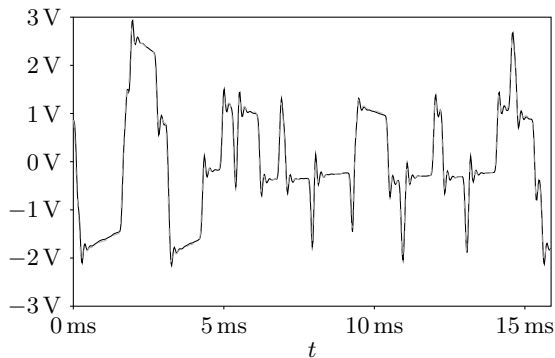


Figure 9: Model output (—) and recorded output (---) for a C_{maj} chord input

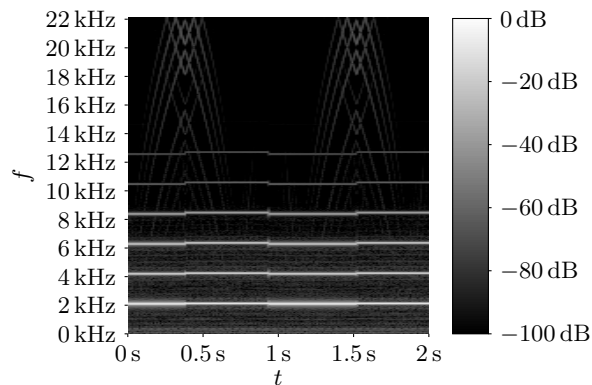
- Instead of recording the BBD clock signal, which would necessitate a very high sampling rate, we reconstruct the clock rate by estimating phase, frequency, and amplitude of a triangular oscillator. Visual inspection of the measurements and simulation results reveals a mismatch in obtained delay time of up to 0.13 ms, varying with time, which is likely due to non-perfect clock rate reconstruction.
- While the filter parameters used are derived from nominal component values, the tolerance of the real components will lead to slightly different filtering behavior.

Figure 9 shows a time domain comparison of the model output and the recorded output when driven with a C_{maj} chord (C_4 , E_4 , G_4). As can be seen, despite the uncertainties mentioned above, very good agreement is achieved. Closer inspection reveals a small time offset (less than 0.04 ms in the shown excerpt) between model output and recording. This impedes interpretation of the difference signal, as it is dominated by peaks around the steep edges of the signal due to the misalignment.

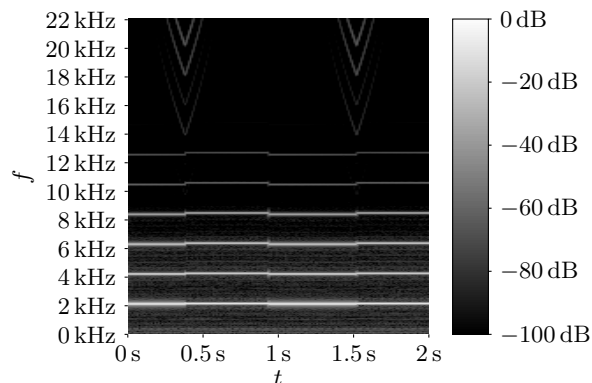
To specifically study the effects of aliasing, the highest note available on the Juno-60, C_7 nominally at 2093 Hz, is used as input. The spectrograms in figure 10 reveal a small amount of aliasing in the recorded output of the analog device (figure 10(c)) and slightly more aliasing in the digital model output at the sampling rate $f_s = 44.1$ kHz (figure 10(a)), as was to be expected.

This extra aliasing in both examples is produced by the assumption of the input to be an impulse-train, as well as the reflection around the audio Nyquist frequency of the image-spectra generated by the sample-and-hold nature of the BBD output. Helped by the existing presence of aliasing in the analog BBD system, this extra aliasing is not audible. In applications where the extra aliasing is problematic, the easiest remedy is oversampling. This is almost tautological, but note that here, a significant portion of the computation happens at the BBD clock rate and is independent of the audio sampling rate, making oversampling especially attractive. The effectiveness can be seen in figure 10(b), where the sampling rate is doubled to $f_s = 88.2$ kHz and the extra aliasing due to the model vanishes.

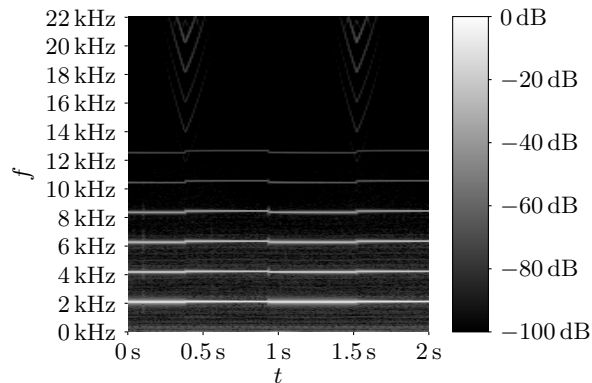
Evaluation based on the Objective Difference Grade (ODG) [9] (advanced mode) as computed with GstPEAQ [10] confirms the high similarity of the simulation to the measurements. Table 2 shows the ODG for the two stimuli discussed above as well as for a



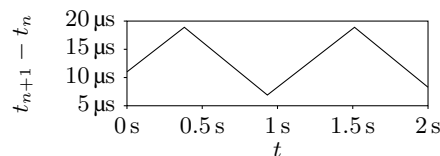
(a) Model output at $f_s = 44.1$ kHz



(b) Model output at $f_s = 88.2$ kHz



(c) Recorded output



(d) Interval between BBD clock edges

Figure 10: Spectrograms of the model output and the recorded output of the BBD output filter in a Juno-60 synthesizer, excited with a C_7 (nominally 2093 Hz), and the LFO-controlled BBD clock edge interval

Table 2: Objective difference grade (ODG) comparing measurement of BBD output and simulation for different stimuli and sampling rates

stimulus	$f_s = 44.1$ kHz	$f_s = 88.2$ kHz
C_2	-0.696	-0.670
C_7	-0.530	-0.393
C_{maj}	-0.646	-0.611

low pitched note, C_2 nominally at 65.41 hertz¹. The ODG ranges between 0 (“differences imperceptible”) and -4 (“differences very annoying”), where -1 corresponds to “differences perceptible but not annoying”. Hence the achieved results could be classified as “differences not annoying if perceptible at all”, with the expected slight improvement for the higher sampling rate. Considering that, as outlined above, the BBD model is not the only source of differences between simulation and measurements, this is a clear success.

5. CONCLUSION

BBD chips sample a signal and delay it by a constant number of sampling intervals. To prevent aliasing from high-frequency content present in the input signal and to suppress image-spectra in the output signal, typical application circuits contain low-pass filters at their input and output. In this paper, we have proposed a model for the combination of the BBD and the filters. In fact, the BBD is trivially modeled as delay-line of constant length, working at the same clock rate as in the analog circuit. The key idea is that the resampling between the audio sampling rate and the BBD clock rate utilizes the filters already existing in the circuit. To this end, the filters are transformed into the digital domain by a modified impulse-invariant transform that allows the output to be taken or the input to be given at arbitrary time instants.

As verified with experimental results, the model thus obtained allows faithful reproduction of the analog system’s behavior, even including aliasing distortion that may occur. However, the audio sampling rate has to be high enough that the filters have sufficient attenuation at the Nyquist frequency. Otherwise, additional aliasing distortion may be introduced. If necessary, this can be trivially prevented by oversampling.

6. REFERENCES

[1] F.L.J. Sangster and K. Teer, “Bucket-brigade electronics: new possibilities for delay, time-axis conversion, and scanning,” *IEEE Journal of Solid-State Circuits*, vol. 4, no. 3, pp. 131–136, jun 1969.

[2] C. Raffel and J. O. Smith, “Practical modeling of bucket-brigade device circuits,” in *Proc. 13th Int. Conf. Digital Audio Effects (DAFx-10)*, Graz, Austria, Sep. 2010, pp. 50–56.

[3] A. Huovilainen, “Enhanced digital models for analog modulation effects,” in *Proc. 8th Int. Conf. Digital Audio Effects (DAFx-05)*, Madrid, Spain, 2005, pp. 155–160.

[4] J. Mačák, “Simulation of analog flanger effect using BBD circuit,” in *Proc. 19th Int. Conf. Digital Audio Effects (DAFx)*, Brno, Czech Republic, 2016.

[5] D. Rocchesso, “Fractionally addressed delay lines,” *IEEE Transactions on Speech and Audio Processing*, vol. 8, no. 6, pp. 717–727, 2000.

[6] V. Zavalishin and J. D. Parker, “Efficient emulation of tape-like delay modulation behavior,” in *Proc. 21st Int. Conf. Digital Audio Effects (DAFx-18)*, Aveiro, Portugal, 2018.

[7] F.L.J. Sangster, “Integrated bucket-brigade delay line using MOS tetrodes,” *Philips Technical Review*, vol. 31, pp. 266, 1970.

[8] J. Pekonen and M. Holters, “Nonlinear-phase basis functions in quasi-bandlimited oscillator algorithms,” in *Proc. 15th Int. Conf. Digital Audio Effects (DAFx)*, York, UK, 2012, pp. 261–268.

[9] ITU Radiocommunication Assembly, *RECOMMENDATION ITU-R BS.1387-1 – Method for objective measurements of perceived audio quality*, ITU, 2001.

[10] M. Holters and U. Zölzer, “GstPEAQ – an open source implementation of the PEAQ algorithm,” in *Proc. 18th Int. Conf. Digital Audio Effects (DAFx)*, Trondheim, Norway, 2015.

¹The evaluated signals are available at <https://www.hsu-hh.de/ant/en/team/martin-holders/dafx2018-bbd>.